Bollettino di Geofisica Teorica ed Applicata Vol. 58, n. 3, pp. 217-232; September 2017
DOI 10.4430/bgta0206

Forecasting the grade-tonnage curves and their uncertainty at the Mehdiabad deposit-Yazd, central Iran

S.A. Hosseini[1], O. Asghari[1], X. Emery[2,3] and M. Maleki[2,3]

[1] *Simulation and Data Processing Laboratory, School of Mining Engineering, College of Engineering, University of Tehran, Iran*
[2] *Department of Mining Engineering, University of Chile, Santiago, Chile*
[3] *Advanced Mining Technology Center, University of Chile, Santiago, Chile*

(Received: April 17, 2017; accepted August 9, 2017)

ABSTRACT The Mehdiabad complex deposit is located 116 km SE of Yazd, in the structural zone of central Iran. At this deposit, important decisions are often based on the grades of multiple elements (zinc, lead, and silver). In this context, it is therefore essential to devise a method that addresses the change of support from the data support to the target smu block, the multivariate nature of the ore control selection criteria and the uncertainty in the actual (unknown) block grades. The solution presented in this study is to employ block-support sequential co-simulation to construct multiple realizations or outcomes of the grade distribution within the deposit that reproduce the natural variability at all spatial scales. The set of realizations allow assessing both grade and tonnage uncertainties and can be used to evaluate the uncertainty on key aspects of the project and transferring uncertainty of the resource/reserve estimates into risk in downstream studies.

Key words: polymetallic deposit, block-support simulation, multiple recoverable metals, spatial uncertainty.

1. Introduction

Recoverable reserve estimation describes the portion of a resource through a mine plan, which is economically and technologically viable, thereby providing the tonnage and grade that are expected to be recovered during mining. This enables calculating and forecasting a recoverable reserve, which is fundamental to the financial success of a mining operation (David, 1977; Peattie and Dimitrakopoulos, 2013) At the feasibility or early production stages, block grade estimates should be conditionally unbiased and have the lowest level of uncertainty. Estimation provides a value that is, on average, as close as possible to the actual (unknown) value, but suffers from an unavoidable smoothing effect that will generally overestimate the tonnage above the economic cut-off and underestimate the corresponding grade for cut-off grades below the mean grade of the ore body (Assibey-Bonsu *et al*., 2015). Stochastic simulation is one of the techniques proposed to correct this smoothing feature. It consists in constructing multiple outcomes (also called realizations) of the ore body that mimic the spatial variability of the true grades, providing a more complete representation of block grade uncertainty, in addition to the uncertainty jointly over

multiple blocks. Simulation methods allow quantifying the uncertainty of the mineral resource and ore reserve prediction risks in downstream studies, such as mine design, mine planning, or operational optimization studies. The risk assessment is achieved by applying transfer functions to the simulation models (Dimitrakopoulos, 2010; Rossi and Deutsch, 2014).

The simulation of mineral resources and ore reserves faces several challenges. On one hand, mine planning is always based on considerations of multiple elements, and the multivariate nature of the ore control selection criteria, as well as the consideration of their joint uncertainty, are common and critical. So, the spatial cross-correlation between elements observed in sampling data needs to be reproduced in simulation models for these to be realistic, for which joint simulation methods are often needed (Goovaerts, 1997). On the other hand, the support effect is a major concern in recoverable reserve estimation, insofar as the volumetric support of the available sampling data (typically, portions of drill holes of a few metres length and a few centimetres in diameter, which can be considered as a quasi-point support) is much smaller than the volumetric support of the selective mining units (smu) or blocks utilized during mining (Parker and Switzer, 1975; Krige, 1976; Armstrong and Champigny, 1989; Sinclair and Vallée, 1994). The usual approach is to simulate the variables of interest at a point support on a fine grid discretizing the entire deposit, then to average the simulated values within the relevant selective mining units so as to obtain a simulation at a block support. This procedure is time consuming and needs a significant amount of computer memory to store all the simulated point-support values. An alternative is direct block-support simulation, which avoids keeping the values simulated onto the discretizing grid in memory. This idea, originally proposed by Journel and Huijbregts (1978), was extended by Boucher and Dimitrakopoulos (2009, 2012) to block co-simulation (i.e., multivariate simulation), by incorporating a de-correlation method (minimum/maximum autocorrelation factors), while Emery and Ortiz (2011) presented two algorithms that significantly increase efficiency and decrease memory requirements during block co-simulation. In addition, block co-simulation was utilized to model porphyry copper deposits (Hosseini *et al.*, 2017).

This paper presents an application of block-support sequential Gaussian co-simulation to forecast the recoverable reserves at Mehdiabad, the biggest zinc, lead and silver deposit in Iran, in which oxide and sulfide domains, controlled by stratigraphy, need to be modelled separately. The following sections include a summary of the co-simulation framework and its extension to block simulation; a thorough description of the deposit and available data; joint simulation of Zn, Pb, and Ag grades in the oxide and sulfide domains, aiming at a geological plausibility of the complex ore body and control on operational quality, required by the mine design and the processing plant. Thereafter, the results from the generated grade-tonnage curves are discussed, followed by conclusions.

2. Block-support sequential Gaussian co-simulation

The following sequential algorithm, proposed by Emery and Ortiz (2011), can be used to simulate K coregionalized variables (such as metal grades) at a block support, based on the Gaussian random field model.

1) For each original variable of interest, the available point-support data are transformed into Gaussian data with a mean of 0 and variance of 1. In the following, the k-th original variable at

a point-support location **x** is denoted by $Z_k(\mathbf{x})$, the associated Gaussian transform is denoted by $Y_k(\mathbf{x})$, while the transformation function, denoted by ϕ_k, is such that:

$$Z_k(\mathbf{x}) = \phi_k\left(Y_k(\mathbf{x})\right) \tag{1}$$

In practice, knowing experimentally the distribution of the variable of interest Z_k, the transformation function ϕ_k can be estimated and modelled by either an expansion into Hermite polynomials (Chilès and Delfiner, 2012) or by piecewise linear and exponential functions (Emery, 2009).

2) Model the joint spatial correlation of the Gaussian data. If there are K Gaussian variables under consideration, then $K(K+1)/2$ experimental covariances or variograms must be calculated and jointly fitted with a theoretical model. The calculation of the experimental covariances or variograms requires identifying the main directions of anisotropy and setting tolerances on the lag separation distances and on the angles (azimuth and dip) defining a direction in space (Goovaerts, 1997; Chilès and Delfiner, 2012). As for the joint fitting, it can be performed by the so-called linear model of coregionalization (LMC) (Goovaerts, 1997; Wackernagel, 2003), which amounts to modelling all the variograms with combinations of the same set of basic variogram models:

$$\boldsymbol{\Gamma}(\mathbf{h}) = \sum_{n=1}^{nst} \mathbf{B}_n \gamma_n(\mathbf{h}) \tag{2}$$

where **h** is a separation vector, **G**(**h**) is the $K \times K$ matrix of direct (diagonal) and cross (off-diagonal) variograms for vector **h**, $\{\gamma_n(\mathbf{h}): n = 1\ldots\text{nst}\}$ is a set of basic variogram models with a unit sill value, and $\{\mathbf{B}_n: n = 1, \ldots, nst\}$ is a set of $K\times K$ symmetric, positive semi-definite matrices, called coregionalization matrices, indicating the contribution of each basic model to the total sill value of the direct and cross variograms. The anisotropy, scale and shape parameters are fitted in the specification of each constituent nested structure $\gamma_n(\mathbf{h})$. Automated or semi-automated procedures can be employed for fitting a linear model of coregionalization with the constraint of positive definiteness of the coregionalization matrices (Goulard and Voltz, 1992; Emery, 2010).

3) Divide the domain targeted for simulation into non-overlapping blocks.

4) Select a block v in the domain among the blocks not yet simulated. Selection can be made according to a random sequence.

5) Discretize v into M points $\{\mathbf{x}_1 \ldots \mathbf{x}_M\}$ and, for $k = 1 \ldots K$, define the k-th original and Gaussian transformed variables at the block support as:

$$Z_k(v) = \frac{1}{M}\sum_{i=1}^{M} Z_k(\mathbf{x}_i) \tag{3}$$

$$Y_k(v) = \frac{1}{M}\sum_{i=1}^{M} Y_k(\mathbf{x}_i) \tag{4}$$

The linear model of coregionalization (Eq. 2) provides the direct and cross covariance functions of the point- and block-support Gaussian variables. For any $k, k' \in \{1 \ldots K\}$, any pair of points **x** and **x´**, and any pair of blocks v and v', we have

- point-to-point covariance:

$$\mathrm{cov}\{Y_k(\mathbf{x}), Y_{k'}(\mathbf{x}')\} = \sum_{n=1}^{nst} \mathbf{B}_n(k,k')(1-\gamma_n(\mathbf{x}-\mathbf{x}')) \tag{5}$$

- point-to-block covariance:

$$\mathrm{cov}\{Y_k(\mathbf{x}), Y_{k'}(v')\} = \frac{1}{M}\sum_{i=1}^{M}\sum_{n=1}^{nst} \mathbf{B}_n(k,k')(1-\gamma_n(\mathbf{x}-\mathbf{x}'_i)) \tag{6}$$

where $\{\mathbf{x}'_1 ... \mathbf{x}'_M\}$ are a set of points discretizing block v'.

- block-to-block covariance:

$$\mathrm{cov}\{Y_k(v), Y_{k'}(v')\} = \frac{1}{M^2}\sum_{i=1}^{M}\sum_{j=1}^{M}\sum_{n=1}^{nst} \mathbf{B}_n(k,k')(1-\gamma_n(\mathbf{x}_i-\mathbf{x}'_j)) \tag{7}$$

where $\{\mathbf{x}_1 ... \mathbf{x}_M\}$ and $\{\mathbf{x}'_1 ... \mathbf{x}'_M\}$ discretize blocks v and v', respectively.

6) Jointly simulate the Gaussian variables at points $\{\mathbf{x}_1 \dots \mathbf{x}_M\}$ within v, constrained by the original point-support Gaussian data and by the previously simulated block-support Gaussian values located in and around block v (this constrained simulation is referred to as a "conditional" simulation in the geostatistical literature). To this end, a non-conditional simulation at points $\{\mathbf{x}_1 \dots \mathbf{x}_M\}$ can be constructed with the well-known LU decomposition of the covariance matrix method (Davis, 1982), and subsequently converted into a conditional simulation by means of a cokriging step (Chilès and Delfiner, 2012, pp. 494-495). For the former stage (non-conditional simulation), as above we simply need to know the direct and cross-covariances of the point support Gaussian variables (Eq. 5), while for the latter stage (conditioning cokriging), the direct and cross-covariances between the point-support and block-support Gaussian variables are needed, according to Eqs. 5 to 7. Simple or ordinary cokriging can be utilized at this stage, depending on whether the mean values of the Gaussian variables are assumed known or not (Emery, 2007, 2009).

7) The average simulated point-support Gaussian values [$Y_k(\mathbf{x}_i)$ with $k = 1 \dots K$ and $i = 1 \dots M$] within block v, give block-support values to be used for further conditioning along the simulation path (step 6):

$$Y_k(v) = \frac{1}{M}\sum_{i=1}^{M} Y_k(\mathbf{x}_i) \tag{8}$$

8) Back-transform the simulated point-support Gaussian values within block v, according to Eq. 1, and average them to obtain simulated block-support values for the original variables:

$$Z_k(v) = \frac{1}{M}\sum_{i=1}^{M} Z_k(\mathbf{x}_i) = \frac{1}{M}\sum_{i=1}^{M} \phi_k(Y_k(\mathbf{x}_i)) \tag{9}$$

Note that the obtained block-support values are not used in the conditioning stage at step 6 and that the block-support Gaussian data (Eq. 8) are used instead.

9) Go back to step 4 until all the blocks are simulated.

Because the simulated point-support Gaussian values do not need to be stored and only block-support information is retained at steps 7 and 8, the above algorithm drastically decreases the memory storage requirements of traditional sequential Gaussian simulation. In addition, the search for nearby conditioning data at step 6 is faster, given that the previously simulated data are considerably fewer when using block-support data instead of point-support data. As an additional

advantage, the algorithm can be applied without any difficulty to partially heterotopic data sets, i.e., data sets for which not all the variables are measured at all the data locations, inasmuch as Gaussian transformation (step 1), covariance or variogram calculation and fitting (step 2) and cokriging (step 6) do not require all the variables to be equally sampled. In the case of entirely heterotopic data sets, the experimental variograms can no longer be calculated and experimental covariances must be used at step 2.

3. Application to the Mehdiabad deposit

3.1. Geological description

The Mehdiabad deposit is a world-class Cretaceous deposit, located 116 km SE of the city of Yazd in the central Iranian tectonic block, one of the most important metallogenic provinces for zinc-lead mineralization (Ghazanfari, 1993; Ghorbani, 2013). The deposit has been explored by various parties since the 1960s. The geologic map of the Mehdiabad area is shown in Fig. 1. Outcrops of the different geological units have been distinguished in the Mehdiabad deposit area, mainly formed by the Sangestan, Taft and Abkouh Formations. The structural geology is characterized by faults that are one of the main controlling factors of mineralization. The Mehdiabad deposit is divided into two parts: 1) the Mountain Ore Body (MOB) (also known as Calamine Mine) that represents the highest parts of the oxide ore mineralization; and 2) the Valley Ore Body (VOB), the main part of the ore body located in a depression surrounded by hills and mountains (Reichert, 2007).

3.1.1. The Mountain Ore Body (Calamine Mine)

The MOB, wedged-in between the Black Hill Fault in the west and the Forouzandeh Fault in the east, is located on a rugged mountainside in the north-western part of the deposit. The MOB is completely oxidized. The oxide ore is hosted by limestone and low magnesium dolomitic limestone (Abkou Formation) that are intensively faulted, brecciated and locally mylonitized (Reichert *et al*., 2003). The oxide ore occurs on three different levels due to tectonic repetition (GSI, 1998). Based on the composition of the sulfide ore of the VOB, the supposed main sulfide mineral association of the MOB domain was galena, sphalerite, barite, and pyrite. However, no clear indications for the sulfide protor of the MOB have been identified, which might be attributed to the thorough oxidation, folding, and faulting of the strata and solution collapse (Reichert, 2007). The most important oxide ore minerals include hemimorphite, hydrozincite, smithsonite, goethite, in addition to small amounts of mimetite, hetaerolite, and sauconite (Reichert *et al*., 2003). Three different stages of ore formation or alteration have been identified: 1) precipitation of stage-1 hemimorphite (and possibly minor smithsonite, hydrozincite, goethite, and hematite) within the fault zones and breccias; 2) alteration of hemimorphite to hydrozincite, and precipitation of goethite/hematite; 3) precipitation of type-2 hemimorphite as mineralization within fractures and open spaces of the fault breccia as well as the oxide ore without significant precipitation of goethite/hematite (Reichert *et al*., 2003).

3.1.2. The Valley Ore Body

The VOB is located in a valley and is covered by an alluvial overburden of about 250 m. The Taft Formation hosts the main portion of the sulfide ore of the VOB (Azari and Sethna, 1994).

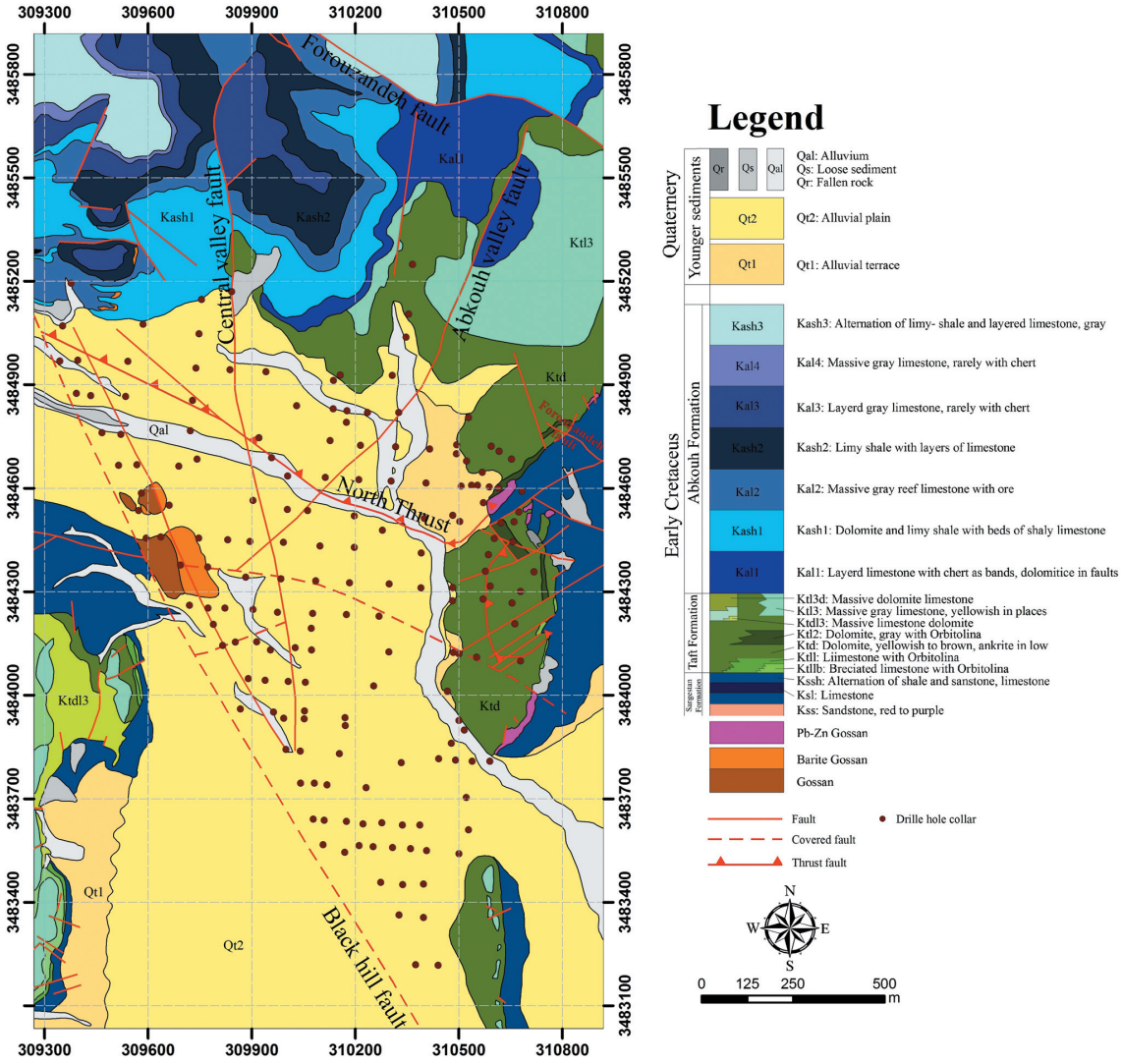

Fig. 1 - Geologic map of the Mehdiabad area.

The strata of the Taft Formation mainly comprise dolomitic and ankeritic limestone, and are characterized by an intensive and extensive brecciation (BRGM, 1994) that is probably the result of emergence, paleo-karstification, and finally, the collapse of these strata (Reichert, 2007). The main portion of the VOB consists of sulfides. The main sulfide minerals are galena, sphalerite, barite, pyrite, and traces of chalcopyrite (Azari and Sethna, 1994), which occur as impregnation of the Taft Formation breccia and as a matrix in a complex fracture and breccia system, and also fill the interstitial space between the breccia fragments (Reichert, 2007). Three different stages of (tectonic or collapse) displacement and mineralization of the valley ore body can be interpreted: 1) paleo-karst and partial collapse of the limestone of the Taft Formation; 2) the dolomitization of the carbonate rock that genetically linked with the emplacement of the sulfide ore and barite; 3) initiated with the oxidation of the sulfide ore that it is still going on (Reichert, 2007).

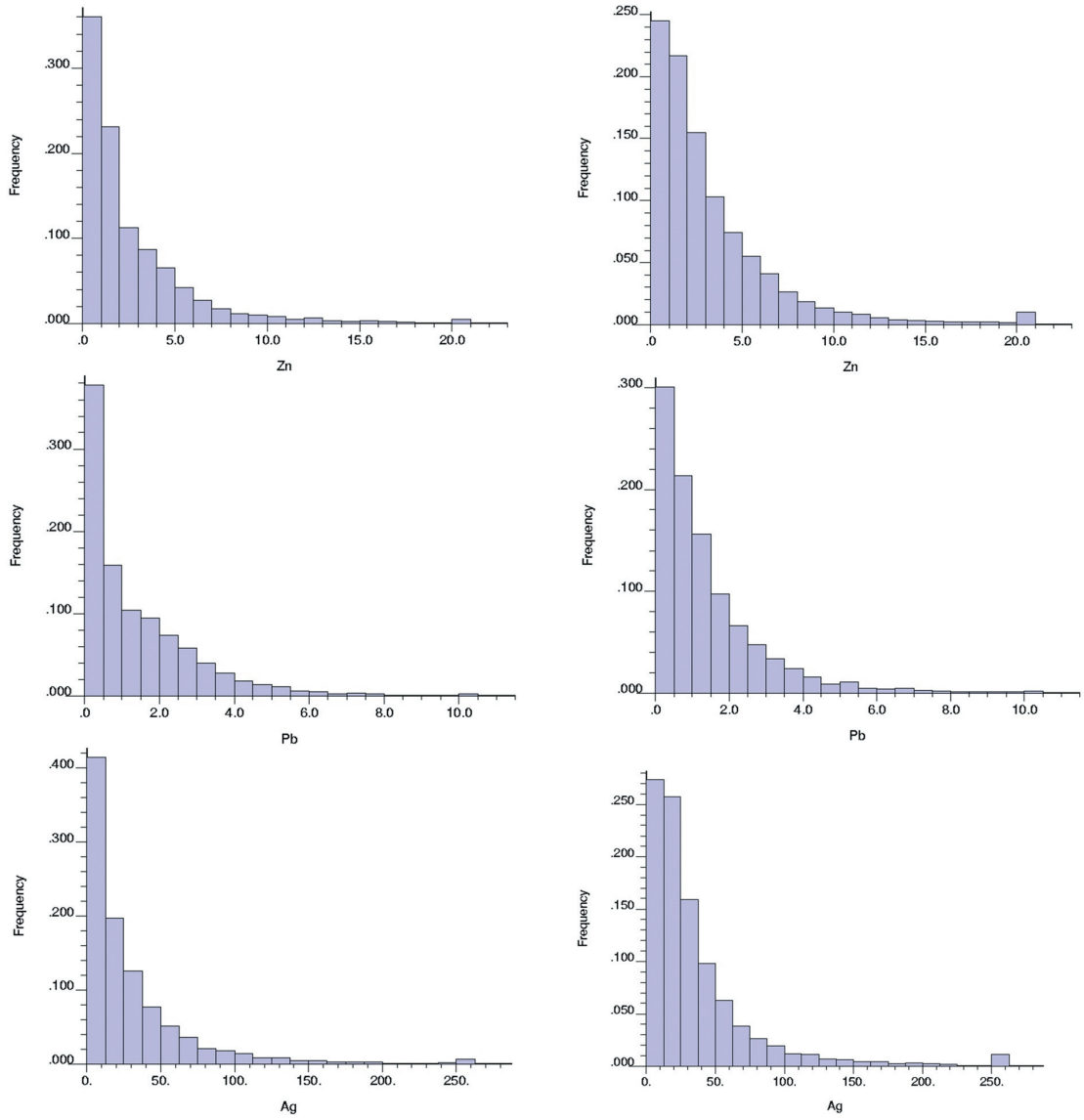

Fig. 2 - Histograms of Zn (%), Pb (%), and Ag (g/t) grade data in oxide (left) and sulfide domains (right).

3.2. Presentation of the data set

The total length of diamond drilling in Mehdiabad is about 55,000 m. Comprehensive geological, structural and geotechnical information was recorded from cores that were composited to a length of 1 m. As the mine geologists claim, the boundaries of the oxide and sulfide mineralization domains were provided by a consulting company and the block-support sequential Gaussian co-simulation was carried out in oxide and sulfide domains separately, using the subset of the composites located within these domains. The grades of three elements (Zn, Pb, and Ag) are considered for this study. The general statistics of the composited data are shown in Table 1 and their histograms are displayed in Fig. 2. It can be seen that the three grades have not been measured for all the samples and the data set is therefore partially heterotopic. The Pearson correlation coefficients are shown in Table 2.

Table 1 - General statistics for the data in the oxide and sulfide domains.

Field	Mean	Std dev	Min	Max	0.25Q	0.50Q	0.75Q	Number
Oxide domain								
Zn (%)	2.741	3.2510	0.0025	27.00	0.686	1.560	3.665	6630
Pb (%)	1.263	1.5066	0	23.24	0.184	0.730	1.882	6626
Ag (g/t)	28.190	40.5850	0	660.00	5.200	14.400	35.794	6461
Sulfide domain								
Zn (%)	3.370	3.8600	0	43.66	1.015	2.220	4.350	9902
Pb (%)	1.259	1.4555	0	23.60	0.298	0.784	1.675	9881
Ag (g/t)	32.25	43.4150	0	825.00	8.633	20.000	39.002	9096

Table 2 - Pearson correlation coefficients between grade variables: oxide domain (upper diagonal) and sulfide domain (lower diagonal).

	Zn	Pb	Ag
Zn	1.000	0.339	0.110
Pb	0.535	1.000	0.616
Ag	0.339	0.600	1.000

Table 3 - Pearson correlation coefficients between variables after Gaussian transformation: oxide domain (upper diagonal) and sulfide domain (lower diagonal).

	Zn	Pb	Ag
Zn	1.000	0.507	0.267
Pb	0.606	1.000	666
Ag	0.411	0.668	1.000

3.3. Block support co-simulation of grades

The following analyses deal with constructing a set of realizations of the zinc, lead, and silver grades over the oxide and sulfide domains of the deposit, which match the known values at the sample locations, reproduce the spatial variability of the true unknown grades at unsampled locations, in addition to the spatial dependence between the grades. The steps to construct these realizations using block-support sequential Gaussian co-simulation are as follows.

1) Declustering of the original data. In unequal sampling cases, declustering weights are primarily used to obtain a representative histogram for each variable (Goovaerts, 1997).
2) A Gaussian transformation was carried out for zinc, lead and silver grades. This nonlinear transformation tends to reduce the influence of outliers, to increase the correlation between variables and to make the estimation of experimental covariance and variograms in subsequent steps of the simulation process more robust (Desbarats and Dimitrakopoulos, 2000). Table 3 shows the Pearson correlation after the Gaussian transformation.
3) The experimental variograms of the Gaussian data are calculated along the horizontal plane (i.e., all the directions with dip 0°, irrespective of their azimuth) and the vertical direction (i.e., the direction with dip 90°), and a linear model of coregionalization is fitted by a semi-automated technique (Goulard and Voltz, 1992). The fitted model is presented in Figs. 3 and

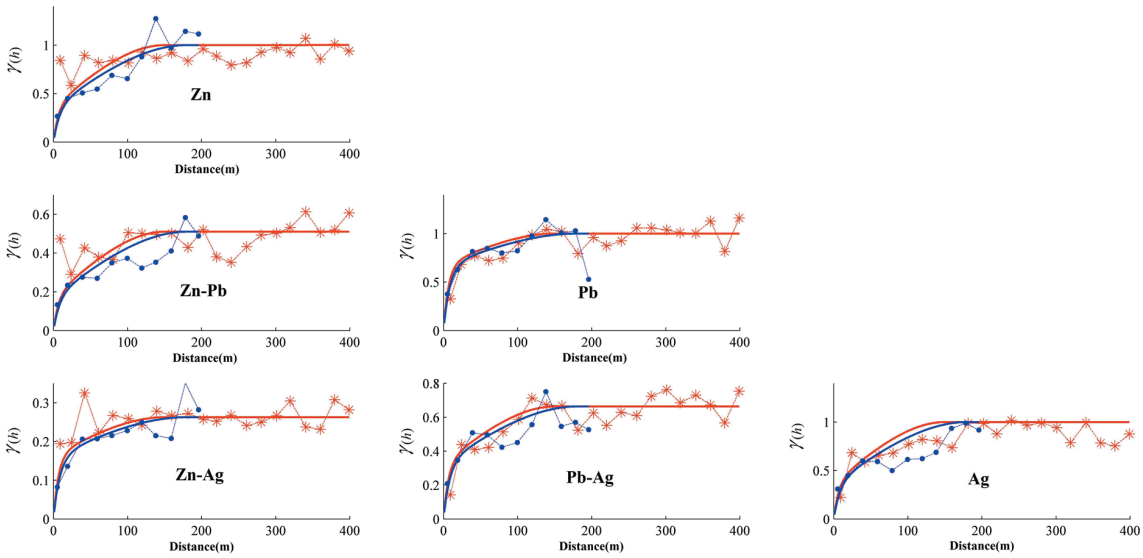

Fig. 3 - Experimental (dashed lines) and modelled (solid lines) direct and cross variograms of Gaussian transforms of zinc, lead, and silver grades, along the horizontal plane (red) and the vertical direction (blue) in the oxide domain.

4 for the oxide and sulfide domains, respectively. The coregionalization model considers three nested structures:

Oxide domain:

i) an exponential variogram with practical ranges of 20 m (horizontal) and 25 m (vertical);
ii) an exponential variogram with practical ranges of 30 m (horizontal) and 80 m (vertical);
iii) a spherical variogram with ranges of 150 m (horizontal) and 180 m (vertical).

The respective coregionalization matrices are found to be as follows:

$$B_1 = \begin{pmatrix} 0.349 & 0.170 & 0.152 \\ 0.170 & 0.659 & 0.329 \\ 0.152 & 0.329 & 0.362 \end{pmatrix}, B_2 = \begin{pmatrix} 0.021 & 0.005 & 0.015 \\ 0.005 & 0.016 & 0.005 \\ 0.015 & 0.005 & 0.010 \end{pmatrix}, B_3 = \begin{pmatrix} 0.630 & 0.332 & 0.100 \\ 0.332 & 0.325 & 0.332 \\ 0.100 & 0.332 & 0.628 \end{pmatrix}$$

Sulfide domain:

i) an exponential variogram with practical ranges of 20 m (horizontal) and 25 m (vertical);
ii) an exponential variogram with practical ranges of 30 (horizontal) and 100 m (vertical);
iii) a spherical variogram with ranges of 150 m (horizontal) and ∞ (vertical).

The respective coregionalization matrices are found to be as follows:

$$B_1 = \begin{pmatrix} 0.573 & 0.397 & 0.273 \\ 0.397 & 0.633 & 0.458 \\ 0.273 & 0.458 & 0.496 \end{pmatrix}, B_2 = \begin{pmatrix} 0.091 & -0.020 & 0.062 \\ -0.020 & 0.137 & -0.018 \\ 0.062 & -0.018 & 0.051 \end{pmatrix}, B_3 = \begin{pmatrix} 0.336 & 0.229 & 0.076 \\ 0.229 & 0.230 & 0.227 \\ 0.076 & 0.227 & 0.453 \end{pmatrix}$$

4) The Zn, Pb, and Ag grades are co-simulated separately in the oxide and sulfide domains using the block-support sequential Gaussian co-simulation method. The results of both domains are subsequently merged. A total of 100 realizations are constructed on 34,054 blocks of size 25×25×10 m located within the ultimate pit limit, representing the smu that

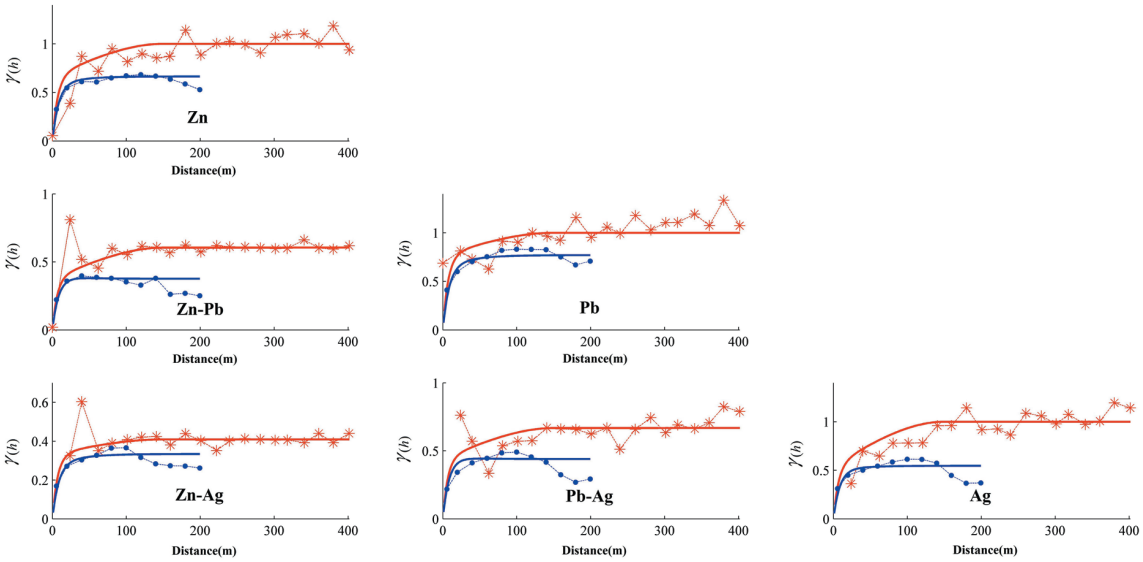

Fig. 4 - Experimental (dashed lines) and modelled (solid lines) direct and cross variograms of Gaussian transforms of zinc, lead, and silver grades, along the horizontal plane (red) and the vertical direction (blue) in the sulfide domain.

will be mined. The block discretization is set to 5×5×2; this discretization level is deemed sufficient, as a finer discretization does not bring much difference in the calculation of point-to-block and block-to-block covariances (Eqs. 6 and 7).

The maps of the first realization for a selected section at 3,484,300 m north are shown in Fig. 5 (left) for zinc, lead, and silver. Also, the corresponding expected values were constructed by averaging the 100 realizations on a block-by-block basis (Fig. 5, right). The latter maps show less contrasts than the former, which is aimed at reproducing the true smu grade variability at

Table 4 - Statistics on simulated grades at block support.

Field	Block model	Mean	Std dev	Min	Max	0.25Q	0.50Q	0.75Q
Oxide domain								
Zn	Realization # 1	2.577	2.026	0.0086	16.865	0.932	1.738	3.014
	Average of all realizations	2.397	1.018	0.2680	10.420	1.757	2.285	2.823
Pb	Realization # 1	1.261	0.894	0.0125	8.133	0.681	1.155	1.785
	Average of all realizations	1.342	0.335	0.3270	2.846	1.131	1.324	1.510
Ag	Realization # 1	28.888	27.330	0.1500	366.061	11.946	22.917	40.09
	Average of all realizations	30.076	11.935	2.1150	91.679	22.061	29.458	36.801
Sulfide domain								
Zn	Realization # 1	3.493	2.091	0.1450	22.247	1.700	2.658	4.053
	Average of all realizations	3.178	0.683	0.5140	8.592	2.802	3.163	3.523
Pb	Realization # 1	1.279	0.806	0.0440	7.926	0.803	1.224	1.791
	Average of all realizations	1.361	0.233	0.3110	3.500	1.240	1.358	1.469
Ag	Realization # 1	39.815	28.815	0.486	403.744	19.250	30.367	47.704
	Average of all realizations	35.408	10.229	5.946	130.815	29.969	35.125	40.657

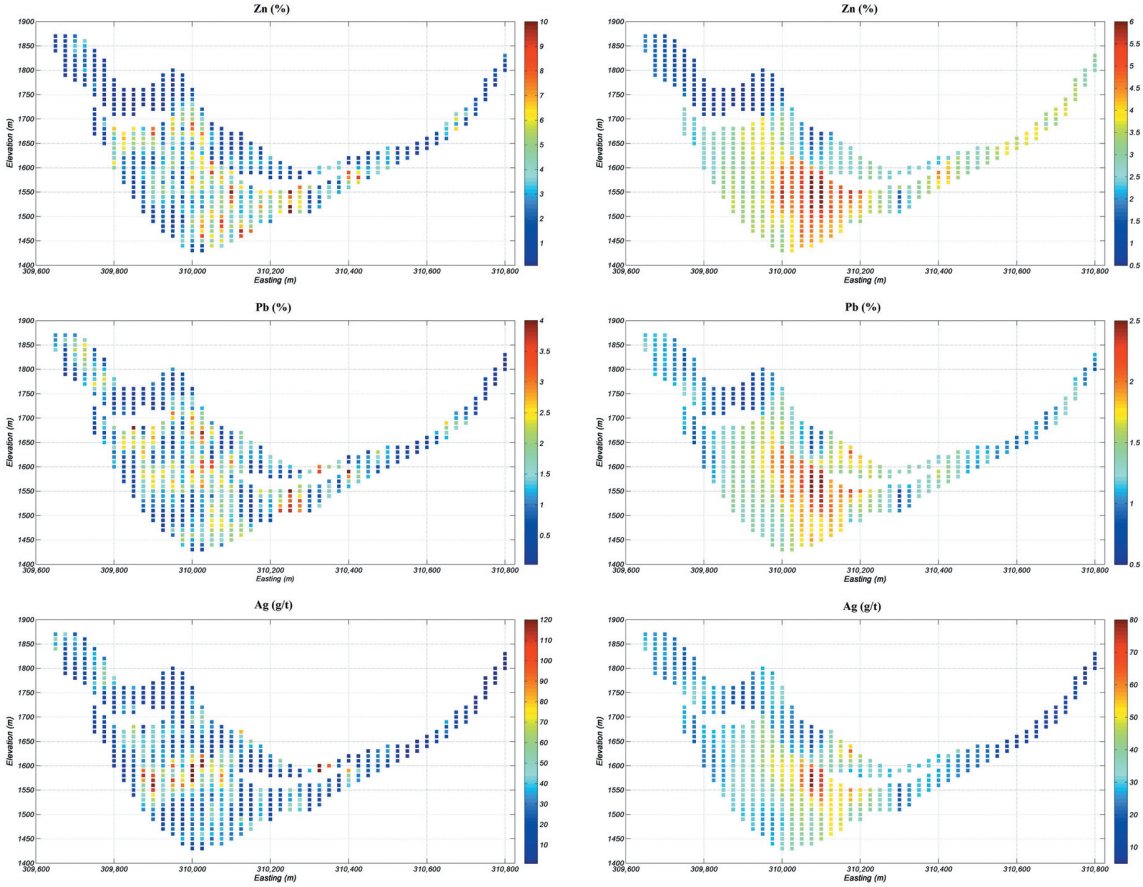

Fig. 5 - Maps of simulated zinc (top), lead (middle), and silver (bottom) block-support grades for realization #1 (left) and maps of expected zinc, lead, and silver grades (average of 100 realizations) (right).

all spatial scales. This fact is corroborated by examining the statistics of the simulated block-support grades, where a higher dispersion and a larger range of the simulated grades for a single realization than for the average of 100 realizations can be observed (Table 4).

The variability of the simulated grades is, nevertheless, smaller than that of the original point-support grades (Table 1), while the mean values are not significantly different between one support and the other, which agrees with the change-of-support theory (Matheron, 1984; Chilès and Delfiner, 2012, pp. 433). The Pearson correlation coefficient between the simulated grades (Table 5) are also higher than that of the original data (Table 2), which is a consequence of the support effect that tends to smooth out the small-scale variability and to improve the correlation between variables.

Table 5 - Pearson correlation coefficients between simulated grades: oxide domain (upper diagonal) and sulfide domain (lower diagonal).

	Zn	Pb	Ag
Zn	1.000	0.576	0.187
Pb	0.634	1.000	0.646
Ag	0.346	0.657	1.000

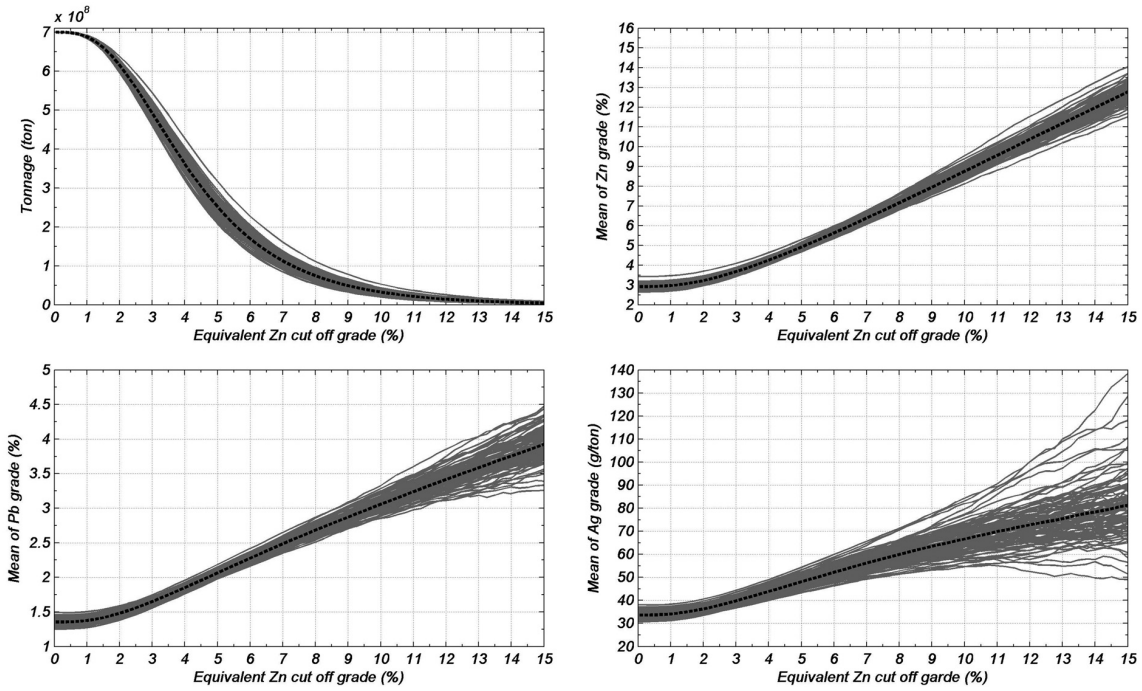

Fig. 6 - Tonnage (top-left), mean zinc grade (top-right), mean lead grade (bottom-left), and mean silver grade (bottom-right) recovered after applying a cut-off on the block-support equivalent zinc grade, calculated for each realization (solid gray lines) and averaged over all the realizations (black dash line).

4. Risk assessment results and discussion

The prediction of the tonnages and grade of ore recoverable with particular selective mining units or blocks is a central problem in mineral resource and ore reserve estimation (Rossi and Deutsch, 2014). In polymetallic deposits, some minerals and different metals can be exploited with an acceptable economic value. The analysis of the uncertainty in grade, tonnage and metal curves by long-term planning engineers can be performed to understand the recoverable mineral resource and ore reserve scenarios at different cut-offs (Hosseini *et al.*, 2017). The Mehdiabad mining project represented a total investment of about 1.3 billion dollars. The high investment, associated with the mineral asset and its metallurgical complexity, highlights the importance of assessing the risks using the jointly simulated variables to ensure the financial viability of the project.

In polymetallic ores, it is common to use a "metal-equivalent grade" to simplify the analysis (Kelmendi and Azemi, 2011). Typically, the contents of minor metals are converted and added to the grade of the major metal with the most stable market price. The equivalence factor for converting the grades of metal 1 and 2 into an equivalent grade is equal to:

$$F_{eq} = \frac{s_1 y_1}{s_2 y_2} \tag{10}$$

$$Z_{eq} = Z_1 + F_{eq} Z_2 \tag{11}$$

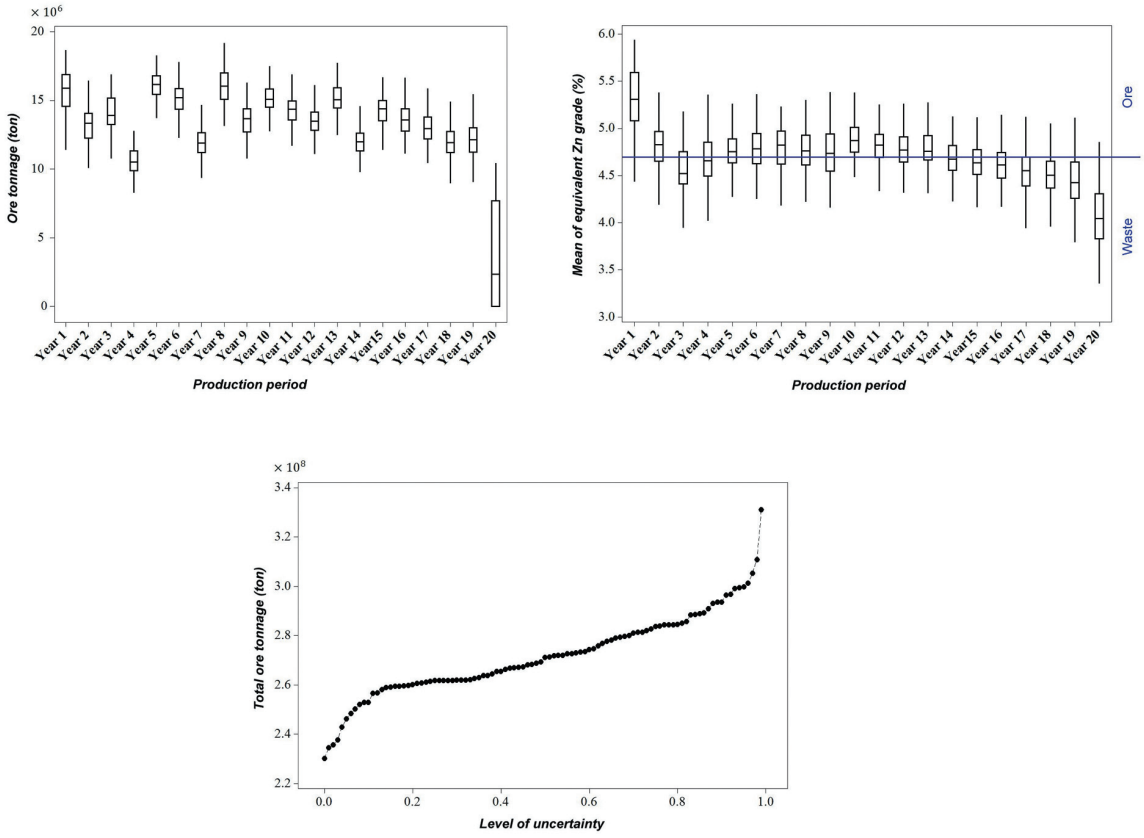

Fig. 7 - Distributions of ore tonnage per production period (top-left), mean equivalent zinc grade per production period (top-right), and overall ore tonnage (bottom), calculated through 100 realizations. Boxplots in the top figures indicate the extremes and the quartiles of the distributions.

where *s* the selling price, *y* the recovery and *Z* the grade for each metal. Note that the weights of metal are *in-situ* and have no mining factors applied to them. In the present case, the equivalent zinc grade for oxide and sulfide types is defined as follows:

Oxide domain:

$$Zn_{eq} = Zn(\%) + (0.956 \times Pb(\%)) + (0.0174 \times Ag(g/t)) \quad (12)$$

Sulfide domain:

$$Zn_{eq} = Zn(\%) + (0.837 \times Pb(\%)) + (0.0152 \times Ag(g/t)) \quad (13)$$

The assumed prices are 0.98 USD/lb for Zn, 0.82 USD/lb for Pb, and 20.29 USD/oz for Ag. A recovery of 63% and 72% was applied to Zn in the oxide and sulfide domains, respectively, 72% was applied to Pb and 40% was applied to Ag (BRGM, 1994).

For each realization, the recoverable zinc, lead, and silver grades above given cut-offs on the equivalent zinc grade are calculated, together with the ore tonnages obtained by considering the average rock density in each mineralization domain, which is derived from a total of 1277

measurements. The expected recoverable grades and tonnages are then defined by an average over the 100 realizations (Fig. 6). As each realization constitutes a plausible outcome for the deposit, the true grade-tonnage curves should lie within the set of simulated curves. The simulated grade-tonnage curves are helpful for ore/waste selection, for resource/reserve classification (Emery *et al*., 2006), for finding the optimum cut-off grade (Osanloo and Ataei, 2003) and for operational and planning purposes (Kelmendi and Azemi, 2011). As an illustration, let us consider a long-term mine plan with 21-year production periods, established by planning engineers, together with an economic cut-off on the equivalent zinc grade equal to 4.7%. The ore tonnage and equivalent zinc grade extracted in each period can be evaluated in each realization. Accordingly, when considering the 100 realizations, one obtains distributions of ore tonnages and grades that quantify the uncertainty on the ore reserves per production period (Fig. 7, top). The overall distribution of ore tonnage (considering the 20 periods) can also be calculated (Fig. 7, bottom), which indicates the quantity of ore to be mined as a function of the level of risk (between 0 to 1).

5. Conclusions

The study shows an application and practical aspects of the block sequential Gaussian co-simulation technique proposed by Emery and Ortiz (2011), which provides efficient forecasting of multiple recoverable metals at the Mehdiabad deposit in central Iran for mine planning and financial assessment. The joint simulation of zinc, lead, and silver grades is performed in the oxide and sulfide domains separately. Such an approach is remarkably simple, as it depends on a few key parameters (essentially, the transformation functions from original to Gaussian variables and the coregionalization model for the Gaussian data), and is capable of handling the change of support from the data to the target SMU supports, the multivariate nature of the ore control selection criteria and the uncertainty in the actual (unknown) block grades. The assessment of global uncertainty of the *in-situ* resources and ore reserves by a set of realizations should be considered in feasibility studies and in supporting important decisions concerning the Mehdiabad project and allow transferring uncertainty of the resource estimates into risk in downstream studies.

Acknowledgements. The third author acknowledges the funding from the Chilean Commission for Scientific and Technological Research, through project CONICYT PIA Anillo ACT1407.

REFERENCES

Armstrong M. and Champigny N.; 1989: *A study on kriging small blocks*. CIM Bulletin, **82**, 128-133.

Assibey-Bonsu W., Searra J. and Aboagye M.; 2015: *The use of indirect distributions of selective mining units for assessment of recoverable mineral resources designed for mine planning at Gold Fields' Tarkwa Mine, Ghana*. J. S. Afr. Inst. Min. Metall., **115**, 51-57.

Azari K. and Sethna S.F.; 1994: *Geology and ore localization study of the zinc-lead sulphide deposit of central Valley Mehdiabad-EH-Bahadoran, Yazd Province, Iran*. In: Proc. 4th Mining Symposium of Iran, Yazd Province, Iran, 223 pp.

Boucher A. and Dimitrakopoulos R.; 2009: *Block simulation of multiple correlated variables*. Math. Geosci., **41**, 215-237, doi:10.1007/s11004-008-9178-0.

Boucher A. and Dimitrakopoulos R.; 2012: *Multivariate block - support simulation of the Yandi iron ore deposit, western Australia*. Math. Geosci., **44**, 449-468, doi:10.1007/s11004-012-9402-9.

BRGM; 1994: *Mehdiabad lead - zinc deposit, prefeasibility study*. Geological Assessment Report, Unpubl. internal report, 119 pp.

Chilès J.-P. and Delfiner P.; 2012: *Geostatistics: modeling spatial uncertainty, 2nd Edition*. John Wiley & Sons, Hoboken, NJ, USA, 734 pp.

David M.; 1977: *Geostatistical ore reserve estimation*, 1st edition. Elsevier Scientific Publishing Company, Amsterdam, The Netherlands, 364 pp.

Davis M.W.; 1982: *Production of conditional simulations via the LU triangular decomposition of the covariance matrix*. Math. Geol., **19**, 91-98.

Desbarats A.J. and Dimitrakopoulos R.; 2000: *Geostatistical simulation of regionalized pore - size distributions using min/max autocorrelation factors*. Math. Geol., **32**, 919-942.

Dimitrakopoulos R.; 2010: *Advances in orebody modelling and strategic mine planning I*. Spectr. Ser., **17**, 345 pp.

Emery X.; 2007: *Conditioning simulations of Gaussian random fields by ordinary kriging*. Math. Geol., **39**, 607-623.

Emery X.; 2009: *Change-of-support models and computer programs for direct block-support simulation*. Comput. Geosci., **35**, 2047-2056.

Emery X.; 2010: *Iterative algorithms for fitting a linear model of coregionalization*. Comput. Geosci., **36**, 1150-1160.

Emery X. and Ortiz J.M.; 2011: *Two approaches to direct block-support conditional co-simulation*. Comput. Geosci., **37**, 1015-1025.

Emery X., Ortiz J.M. and Rodríguez J.J.; 2006: *Quantifying uncertainty in mineral resources by use of classification schemes and conditional simulations*. Math. Geol., **38**, 445-464.

Ghazanfari F.; 1993: *Zn - Pb mines and deposits in Iran*. M. Sc. thesis, University of Tehran, Iran, 199 pp.

Ghorbani M.; 2013: *The economic geology of Iran: mineral deposits and natural resources*. Springer Science Business Media, Dordrecht, The Netherlands, 581 pp., doi:10.1007/978-94-007-5625-0.

Goovaerts P.; 1997: *Geostatistics for natural resources evaluation*. Oxford University Press, Oxford, UK , 483 pp.

Goulard M. and Voltz M.; 1992: *Linear coregionalization model: tools for estimation and choice of cross-variogram matrix*. Math. Geol., **24**, 269-286.

GSI (Geolgical Survey of Iran); 1998: *Geological studies on the Mehdi Abad lead and zinc project*. Unpubl. Report.

Hosseini S.A., Asghari O. and Emery X.; 2017: *Direct block-support simulation of grades in multi-element deposits: application to recoverable mineral resource estimation at Sungun porphyry deposit*. J. South Afr. Inst. Min. Metall., **117**, 577-585, doi:10.17159/2411-9717/2017/v117n6aB..

Journel A.G. and Huijbregts C.J.; 1978: *Mining geostatistics*. Academic Press, London, UK, 600 pp.

Kelmendi S. and Azemi F.; 2011: *Comparative economic elements of mineral resources in the context of international management*. Tranzicija, **13**, 47-56.

Krige D.G.; 1976: *A review of the development of geostatistics in South Africa*. In: Proc. Geostat 75, Advanced geostatistics in the mining industry, pp. 279-293.

Matheron G.; 1984: *The selectivity of the distributions and the second principle of geostatistics*. In: Verly G., David M., Journel A.G. and Marechal A. (eds), Geostatistics for Natural Resources Characterization., Reidel, Dordrecht, The Netherlands, pp. 421-433.

Osanloo M. and Ataei M.; 2003: *Using equivalent grade factors to find the optimum cut-off grades of multiple metal deposits*. Miner. Eng., **16**, 771-776.

Parker H.M. and Switzer P.; 1975: *The statistics of selective mining*. Stanford University, Stanford, CA, USA, Report n. EFS NSF 75, 26 pp.

Peattie R. and Dimitrakopoulos R.; 2013: *Forecasting recoverable ore reserves and their uncertainty at Morila gold deposit, Mali: an efficient simulation approach and future grade control drilling*. Math. Geosci., **45**, 1005-1020.

Reichert J.; 2007: *A metallogenetic model for carbonate-hosted non-sulphide zinc deposits based on observations of Mehdi Abad and Irankuh, central and southwestern Iran*. Ph.D. Thesis, University Halle Wittenberg, Halle, Germany, 279 pp.

Reichert J., Borg G. and Rashidi B.; 2003: *Mineralogy of calamine ore from the Mehdi Abad zinc–lead deposit, central Iran*. In: Proc. 7th Conference SGA Meeting, Athens, Greece, Vol. Mineral Exploration and Sustainable Development, pp. 97-100.

Rossi M.E. and Deutsch C.V.; 2014: *Mineral resource estimation*. Springer, Dordrecht, The Netherlands, 332 pp.

Sinclair A.J. and Vallée M.; 1994: *Improved sampling control and data gathering for improved mineral inventories and production control*. In: Dimitrakopoulos R. (ed), Geostatistics for the next century, Quantitative geology and geostatistics, Springer, Dordrecht, The Netherlands, pp. 323-329.

Wackernagel H.; 2003: *Multivariate geostatistics: an introduction with applications, 3rd edition*. Springer-Verlag, Berlin, Germany, 388 pp.

Corresponding author: Omid Asghari
Simulation and Data Processing Laboratory, School of Mining Engineering
University College of Engineering, University of Tehran, Tehran, Iran
Phone: +982188008838; fax: +982188008838; e-mail: o.asghari@ut.ac.ir